RASĀYAN *J. Chem.*
Vol. 17 | No. 3 |838-847| July - September | 2024
ISSN: 0974-1496 | e-ISSN: 0976-0083 | CODEN: RJCABP
http://www.rasayanjournal.com
http://www.rasayanjournal.co.in

CHARACTERIZATION OF NANO-DOPED LIQUID CRYSTALS BY X-RAY DIFFRACTION, SCANNING ELECTRON MICROSCOPE AND OPTICAL COLORIMETRY

SowmyaMudunuru[1], Ganapavarapu Veera Raghava Sharma[1,✉] Chandra Sekhara Rao Gurubilli[1], Srinivasa Rao G.[1]and Gowri Sankara Rao B.[2]

[1]Department of Chemistry, GITAM School of Science, GITAM Deemed to be University, Visakhapatnam-530045, Andhra Pradesh, India.

[2]Department of Physics, Scholl of Sciences, Godavari Global University, Rajahmundry - 533296, Andhra Pradesh, India.

✉Corresponding Author: sganapav@gitam.edu

ABSTRACT

In this paper, the self-assembling nature of nano-doped liquid crystals is characterized using different techniques. Liquid crystals, namely 4, n-alkoxybenzoic acid (nOBA, where n = 7,8), doped with magnetic nanoparticles (Fe_3O_4 of size 20nm) are considered for the present study. The structural and morphological properties of nano-doped liquid crystals are determined by the techniques of X-ray diffraction and Scanning Electron Microscopy. Morphological properties like grains, grain boundaries, and crystal defects are elucidated using the scanning electron microscope technique. Structural properties such as crystal structure, grain size, inter-atomic spacing, lattice constant, and dislocation density are determined using X-ray diffraction studies. The characteristics measured from the X-ray diffraction studies are correlated using the statistical analysis of Scanning electron microscope images. This is an objective analysis of X-ray diffraction studies. In addition to these techniques, colorimetric studies of optical anisotropic liquid crystals are carried out by measuring the chromaticity coordinates and color purity. This study utilizes the polarizing optical microscope technique. Furthermore, the influence of nano dopants on the characteristics of liquid crystals with carbon chain length is also discussed.

Keywords: Liquid Crystals, Nanoparticles, X-ray diffraction, Scanning Electron Microscope, Polarizing Optical Microscope.

RASĀYAN*J. Chem.*, Vol. 17, No.3, 2024

INTRODUCTION

Recent research has shown a rapid expansion in the field of liquid crystal nanocomposites, as it offers great potential for designing and developing novel materials for a variety of applications.[1-3] The process of doping various nanomaterials onto liquid crystal samples is highly efficient and results in the formation of diverse liquid crystal nano composites. The self-assembled nature of these liquid crystal nanocomposites controls the structural and physical properties of materials and improves material performance for device applications. Carbon nanotubes and graphene flakes form long-range orientational ordered structures and modify the liquid crystals (LCs) optical, electro-optical, and dielectric anisotropies, which will be useful for the development of devices in electronics, optoelectronics, fabricating electromechanically coupled devices, etc.[4-6] Metal oxide dopants have received significant attention among various nanoparticle dopants due to their ability to adopt versatile structural geometries. This characteristic makes them valuable tools in the development of novel materials.[7-9] Thus, incorporating liquid crystalline compounds into metal oxide nanoparticles enhances the efficacy of the liquid crystalline material and expands its potential uses in optical information processing systems, display technology, microscopy, biology, drug design, and medicine.[9-12]Current research utilizes 20nm magnetic nanoparticles (Fe_3O_4) as dopants, while 4, n-alkoxybenzoic acids (nOBA, where n = 7,8) have been employed as the base mesogenic material. For a long time, nOBA liquid crystal compounds have been utilized as building blocks for other liquid crystalline compounds, but a relatively small number of studies on the dispersion of nanoparticles in 4, n-alkoxybenzoic acids have been reported. Here, the self-assembling nature of magnetic nanoparticles (Fe_3O_4) with nOBA liquid crystals forms the supramolecular nanocomposites,

http://doi.org/10.31788/RJC.2024.1738868

which are abbreviated as NnOBA (where n = 7, 8). The type and extent of interaction between the guest magnetic nanoparticles (Fe_3O_4) and nOBA affect the morphological, structural, and physical characteristics of liquid crystals.[12-15]Such properties are characterized using different experimental and computational techniques. Structural characterization of liquid crystals is done using X-ray diffraction analysis, and morphological characterization is done using scanning electron microscopy (SEM). Morphological properties like grains, grain boundaries, and crystal defects are elucidated using the SEM technique.[16,17] Structural properties such as crystal structure, grain size, inter-atomic spacing, lattice constant, and dislocation density are measured using X-ray diffraction studies.[18,19] The characteristics measured from the X-ray diffraction studies are correlated using the statistical analysis of scanning electron microscope images. This is an objective analysis of X-ray diffraction studies. The correlation study is done by means of computing some statistical parameters from SEM image data or intensity values. Such statistical parameters include Homogeneity and edge density. They are computed on the MATLAB platform.[20,21]In addition to these techniques, colorimetric studies of optical anisotropic liquid crystals are carried out by measuring the chromaticity coordinates and color purity of samples. This was done using the polarizing optical microscope technique. Chromacity coordinates give information about the color or wavelength of light being absorbed, transmitted, or emitted when a sample undergoes any chemical reaction or change.[22,23] Generally, this kind of characterization can be done using the UV-visible Spectrophotometric technique and the photo luminance technique.[24,25] But in the case of liquid crystals, due to their high optical anisotropy, the changes in color intensity values or wavelengths of light being absorbed or transmitted can be observed using the polarizing optical microscope technique. These observations can be recorded as beautiful textures as a function of temperature. Therefore, the chromaticity coordinates and color purity of the liquid crystals and their nanocomposites are computed from the optical textures of the liquid crystals and will be used for the colorimetric study of samples. The obtained chromaticity coordinates and color purity will be compared with the standard chromaticity diagram.[22,23,26]

EXPERIMENTAL

Sigma-Aldrich laboratories in the USA provided us with the necessary chemical ingredients for our study. These included 4, n-alkoxy benzoic acid (nOBA, where n=7,8) and Ferric oxide (Fe_3O_4) nanoparticles. The magnetite (Fe_3O_4) nanoparticles had a size of 20 nm and were used at a weight percentage of 0.5% for doping purposes. The magnetite nanoparticles were added to the isotropic liquid phase of our liquid crystal material, which consisted of 4, n- alkoxy benzoic acid. This mixture was then continuously stirred for approximately 3 hours. After cooling, we were left with nano-doped forms of 4, n-alkoxybenzoic acids (nOBA), which were then thoroughly studied in our research. The powder samples were subjected to X-ray diffraction analysis using a Powder X-ray diffractometer, Bruker, and D8 Advanced model. The resulting images were captured in grayscale with a resolution of 519 x 268 and intensity values ranging from 0 to 255 for subsequent analysis. This analysis was performed through the use of MATLAB (R2013) software, running on a P5 1.6GHz computer with 2GB of RAM, as detailed in references.[20,21] The methods utilized in this investigation are described in the following section. Colorimetric studies were conducted using optical texture images acquired from an SD-Tech polarizing optical microscope equipped with a hot stage and camera attachment.[27]

Theoretical Considerations

SEM and X-ray diffraction analysis are the two primary tasks involved in the characterization of newly synthesized nanostructure materials. SEM analysis gives information about the morphological qualities of the materials while X-ray diffraction analysis gives structural information. Colorimetric studies give information about the color response of the materials.

Computation of Statistical Parameters from Sem Images

Important characteristics for the correlation investigations of SEM with X-rd are the intensity values of grain and grain boundaries in the SEM images. Here, by examining the grains and grain boundaries in SEM images, statistical parameters are derived from the grey-level intensity values of the images. A set of statistical parameters was derived from this study by looking at the features at each pixel in the image.[20, 21] S (*m, n*) is an SEM image with the horizontal and vertical coordinates of *m* and *n.* It is a two-dimensional

function with x pixels in the vertical direction and y pixels in the horizontal direction. The formula for the total number of pixels is ($x*y = N$), and the following describes the statistical characteristics.

Homogeneity Measurement

The degree of uniformity, or closeness, between the values in the image's distribution is measured by homogeneity. Only a small range of grey levels, but a reasonably high probability *(P(m, n)),* are present in homogeneous textures. As a result, the square will be large. Homogeneity takes into account the likelihood that intensity-value pairings may occur.

$$Homogeneity = \sum_{m=1}^{x}\sum_{n=1}^{y}(P(m,n))^2 \quad (1)$$

In this case, the image's grey-level co-occurrence matrix is used to measure homogeneity. The associations between a pixel's intensity and its surrounding pixels are represented by the GLCM's elements.[20,21, 28]

Edge Density Measurement

Edge density quantifies the gradient magnitude of edges throughout a neighborhood, while edges themselves are the discontinuity in the intensity values. As defined in[29],

$$Edgedensiy = \frac{\sum W}{N} \quad (2)$$

Where N is the total number of pixels (width * height) and W is the number of white pixels.

Calculation of Structural Parameters from XRD Patterns

By utilizing X-ray diffraction peaks, the following structural parameters of crystalline solids can be measured.[18,19,30,31]

Grain Size

The Scherrer formula is used to determine the grain size (D).

$$D = \frac{0.94\lambda}{\beta\cos\theta} \quad (3)$$

Where λ is the Bragg angle, β is the FWHM, and 1.5406 A^0 is the utilized X-ray wavelength.

Lattice Constant

The following formula was used to determine the lattice constant.

$$a = d\sqrt{h^2+k^2+l^2} \quad (4)$$

"*a*" is the lattice constant, "*h, k,* and *l*" are Miller indices, and "*d*" is the interplanar distance.

Dislocation Density

The length of the dislocation lines or the number of dislocations per unit volume of the crystal is measured by the dislocation density (δ), which was computed using the equation.

$$\delta = \frac{1}{D^2} \quad (5)$$

Here, grain size D is determined using the Sherrer formula.

The defined parameters are very responsive to variations in the morphological and structural attributes.

Colorimetric Studies

Chromacity coordinates and Color purity are the important parameters for the colorimetric study of liquid crystal samples. The CIE convention states that the amount of light that is continuously transmitted or reflected from a surface is represented by the parameter called color purity, and the color impression of the object in human vision is described by the parameter called chromaticity coordinates. The tristimulus values of the image are used for determining the chromaticity coordinates of any color image, including liquid crystal textures. i.e., from the R, G, and B main color components. They are the ratio of one tristimulus over the sum of all three tristimulus values. They are defined as follows:[32,33]

Chromacity coordinates (*x,y*)

$$x=\frac{R}{R+G+B};\ y=\frac{G}{R+G+B}. \quad (6)$$

Where the monochromatic picture planes (R, G, and B) are derived from the RGB color image. Three colors are added together to provide the majority of the visible spectrum's colors. The equation provides the color purity based on these coordinates.[22, 23]

$$\text{color purity} = \frac{\sqrt{(x-x_i)^2+(y-y_i)^2}}{\sqrt{(x_d-x_i)^2+(y_d-y_i)^2}} * 100\% \quad (7)$$

Where the CIE chromaticity coordinates of the sample, white illumination, and dominant wavelength are shown, respectively, by (x, y), (x_i, y_i), and (x_d, y_d). The parameters that have been established exhibit sensitivity to variations in the textural characteristics of liquid crystals in relation to temperature and wavelength. Here also, the computational tool MATLAB is used to compute chromaticity coordinates and color purity.

RESULTS AND DISCUSSION

The structural, morphological, and colorimetric studies of supramolecular nanocomposites such as magnetic nanoparticles (Fe_3O_4) doped with 4, n alkoxy benzoic acids (NnOBA, where n=7,8) are characterized using X-rd, SEM, and POM techniques.

SEM Analysis

The recorded scanning electron microscopic images of nano-doped liquid crystal NnOBA (where n=7,8) are shown in Fig.-1. Utilizing these observed data, the surface morphology of the nano systems is investigated.

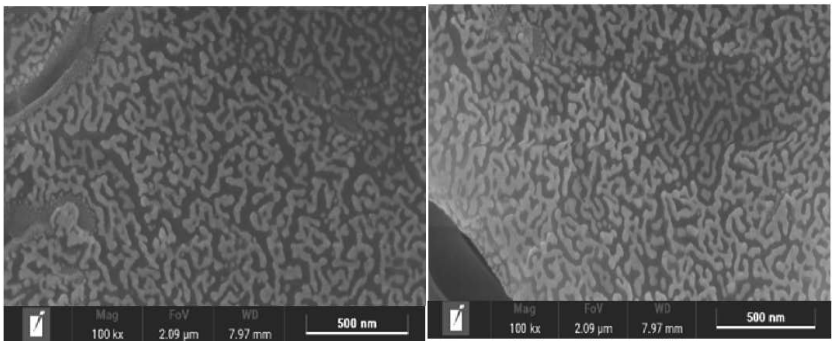

(a) (b)

Fig.-1: SEM Images of Liquid Crystal Nanocomposites (a)N7OBA; (b)N8OBA

From Fig.-1, it was evident that there are spherical grains and traces of empty sites in nano-doped liquid crystals. Fe_3O_4 doping changes the liquid crystal's surface and creates a densely packed structure with distinct grains and grain boundaries. This allows variations in the molecular alignment, which leads to the formation of new phases in nano-doped systems from pure compounds. Statistical analysis of these SEM images also provides information about the morphology of nano-doped liquid crystals. This was done by computing the parameters: edge density and homogeneity. Homogeneity measures the surface uniformity, and edge density measures the discontinuities in the intensity values due to the grin boundaries. These parameters are measured from the spatial distribution of gray-level intensities of SEM images obtained due to electron transmission and reflections. These electron transmissions and reflections are related to the structural properties of liquid crystals. Homogeneity and Edge density of the SEM images are computed using Eqs. (1, 2). The obtained values of nano-doped liquid crystals are given in Table-1.

Doping of Fe_3O_4 nanoparticles modifies the surface of the liquid crystal material and leads to variations in the transmitted intensity values of SEM images. From Table-1, it was observed that the liquid crystal nanocomposites N8OBA have a low value of homogeneity compared to N7OBA. The density of the liquid crystal molecules at the surface and the length of the alkoxy chain could be the cause of this. For the nano system N8OBA, the long liquid crystal molecules that connect the various grain sizes and grain

boundaries form a tight packing structure that produces high surface roughness and with different gray level intensity values.

Table-1: Statistical Parameters Computed from the SEM Images of NnOBA (where n=7,8)

Compound	edge density	Homogeneity
N7OBA	0.231	0.850
N8OBA	0.246	0.789

Edge density is another significant statistical metric that is used to examine the morphological characteristics of SEM images of nano systems. All those edges are breaks in the intensity values, which are referred to as defects. The gradient of the edges that are defined by the grain boundaries is all that makes up edge density. Higher or lower edge densities result from discontinuities in intensity values caused by surface recombination of distinct grains and grain borders caused by doping. This allows for structural defects in liquid crystals. Here, doping of Fe_3O_4 modifies the alignment of molecules at the surface of the liquid crystal material and results in some discontinuities in the intensity values. This can be observed as the induction of new phases in nano-doped liquid crystals from pure compounds using Polarizing optical Microscope (POM). The discontinuities in the intensity values are reduced, and the edge density is lowered by surface recombination with large sized grains and grain boundaries. Here, liquid crystal nanocomposites N8OBA have a high value of edge density compared to N7OBA.

X-Ray Diffraction Studies of Noba, Innova

Structural parameters of pure 4, n alkoxy benzoic acids (nOBA) and (Fe_3O_4) doped 4, n alkoxy benzoic acids (NnOBA, where n = 7, 8,) are studied from the X-ray diffraction patterns. The representative X-ray diffraction pattern of 7OBA and its nanocomposites, N7OBAis shown in Fig.-2.

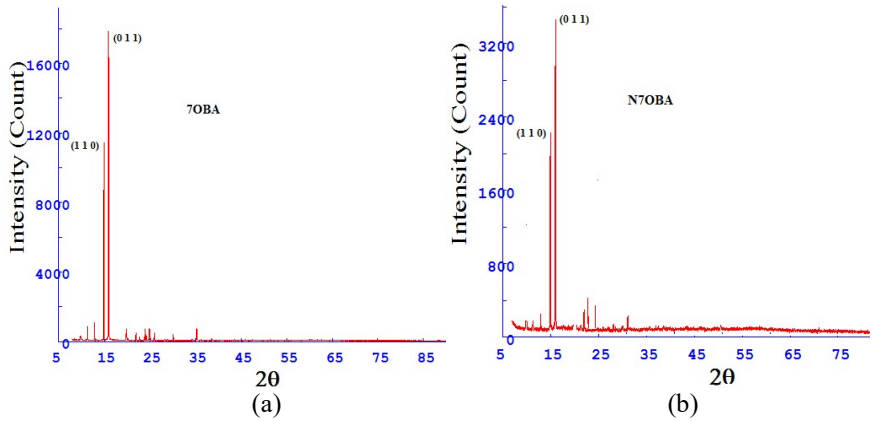

Fig.-2: X-ray Diffraction Patterns of (a) Pure 7OBA and (b) Fe_3O_4Doped 7OBA (N7OBA)

According to X-ray diffraction studies, the molecules in the nOBA (where n = 7,8) liquid crystals have a structural symmetry of monoclinic with diffraction peaks at values of 14.91^0, 15.997^0 for 7OBA, and 14.77^0,16.29^0 for 8OBA. They were indexed as (1 1 0), and (0 1 1) planes.[30] Further, no significant peaks have been identified. Similarly, the molecules in the NnOBA liquid crystals also have the same structural symmetry as monoclinic, with slight shifts in diffraction peaks at values of 14.953^0, 16.018^0 for N7OBA, 14.8^0, 16.80^0 for N8OBA, and were indexed the same as nOBA planes (1 1 0), (0 1 1). This suggests that both pure and nano systems exhibit the same structural symmetry and preferential orientation along the (1 1 0) and (0 1 1) directions even after doping. However, the intensities of the high diffraction peaks are observed with decreasing intensity compared to the nOBA. This right-hand side shift of the Bragg angle and decreasing intensity of diffraction peaks demonstrate that the incorporation of Fe_3O_4 dopants in the nOBA causes the lattice strain and some orientational defects in the molecular structure. This was confirmed by the thermal analysis technique for liquid crystals.[34, 35] The defined structural parameters of pure and nano-doped liquid crystalline systems are measured from Eqs: 3-5 and are tabulated in Table-2.

Table-2: Structural Parameters Calculated for h k l Planes (1 1 0), (0 1 1) from the X-rd Patterns ofPure nOBA and Fe_3O_4Doped nOBA (NnOBA, Where n=7,8) *(0 1 1) plane*

Structural parameters	7OBA	N7OBA	8OBA	N8OBA
Grain size(nm)	631	489	213	206
interatomic spacings (A°)	5.92(5.53)	5.91(5.52)	6.0(5.43)	5.9(5.26)
lattice parameter	8.372(7.82)	8.37(7.80)	8.5(7.67)	8.45(7.43)
dislocation density*10^{12}	2.7(0.418)	4.1(0.94)	21.6(2.61)	23.4(3.33)

Table-2 gives the structural parameters of pure (nOBA) and nano-doped liquid crystals (NnOBA, where n = 7, 8). The grain size of nano systems: NnOBA is small compared to the pure compounds. The grain sizes for NnOBA (where n = 7, 8) is 489nm,206 nm, and for pure compounds (7OBA and 8OBA), they are 631nm and 213nm. The doping of Fe_3O_4 in nOBA results in a notable difference in the grain size of pure and nanocomposite liquid crystals. Generally speaking, tiny grain size results in reduced surface smoothness for the materials, increasing material efficiency. Parameters such as interatomic spacing and lattice parameters of nano-doped liquid crystals (NnOBA) are lower than those of pure compounds (nOBA). The doping of Fe_3O_4 nanoparticles causes a decrease in interatomic spacing, which accounts for the modest contraction of the lattice parameter in pure liquid crystals. However, the values of the lattice parameter and inter-atomic spacing for the nano system N8OBA were small compared to N7OBA. This may be due to the length of the alkoxy chain and the density of the liquid crystal molecules at the surface. The presence of nano dopant at the surface of the liquid crystals has the ability to enhance the stability of the lattice. The same can be observed for the compounds with increasing chain lengths (n = 7,8). Another parameter called dislocation density is high for liquid crystal nanocomposites compared to pure compounds. This is because strong H-bonding between the molecules of 4, n-alkoxybenzoic acid creates an obstacle to the appropriate dispersion of nanoparticles and permits a greater number of dislocation lines in liquid crystal composites. This leads to a high value of dislocation density. The structural parameters, dislocation density, and grain size, more closely resemble and correlate to the statistical parameters of SEM images. Such parameters include edge density and homogeneity. In SEM analysis edge density is nothing but the discontinuity in the intensity values due to the surface modification, and in X-rd studies, dislocations are structural defects due to the surface modification by doping or dispersion of nanoparticle. Here, both parameters relate to the defects in liquid crystals. The structural and statistical parameters of the nano-doped liquid crystals are plotted as a function of carbon chain length and are shown in Fig.-3.

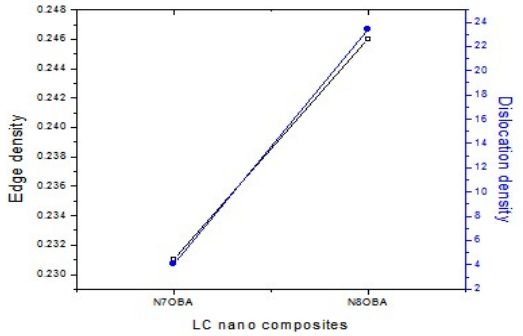

Fig.-3: Statistical Parameter Vs Structural Parameter

Grain size and homogeneity are another set of correlation parameters for statistical analysis (SEM and X-RD). If the grain size is small, it gives a high surface roughness to the liquid crystal material. Similarly, if the homogeneity of the SEM image is lower, the intensity values allow for high surface roughness. The above observations demonstrate that the liquid crystal nanocomposites N8OBA have significant structural and morphological parameters compared to N7OBA.

Colorimetric Studies of nOBA and NnOBA, (where n=7,8)

Colorimetric studies of the optical anisotropic liquid crystals nOBA and NnOBA (where n = 7, 8) are carried out by measuring the chromaticity coordinates and color purity of samples. Using POM, the

optical anisotropy of given materials can be observed as beautiful textures, and the analysis of those textural intensities is useful for the colorimetric studies of liquid crystals. Liquid crystals nOBA (where n = 7, 8) exhibit the enantiotropic Smectic C and Nematic phases. The dispersion of Fe_3O_4 nanoparticles within nOBA liquid crystals yields self-assembled nanocomposites, specifically N7OBA and N8OBA. The incorporation of Fe_3O_4 in nOBA leads to the suppression of the smectic C phase in 7OBA and 8OBA, resulting in the formation of a smectic A phase in N7OBA and a cholesteric phase in N8OBA. However, the nematic phase remains unaffected by this complexation. Fig.-4-5 displays the textures of both pure and nanocomposite samples.

(a) (b)

Fig.-4: Nematic Phases and Smectic C Phase of nOBA (where n=7,8)

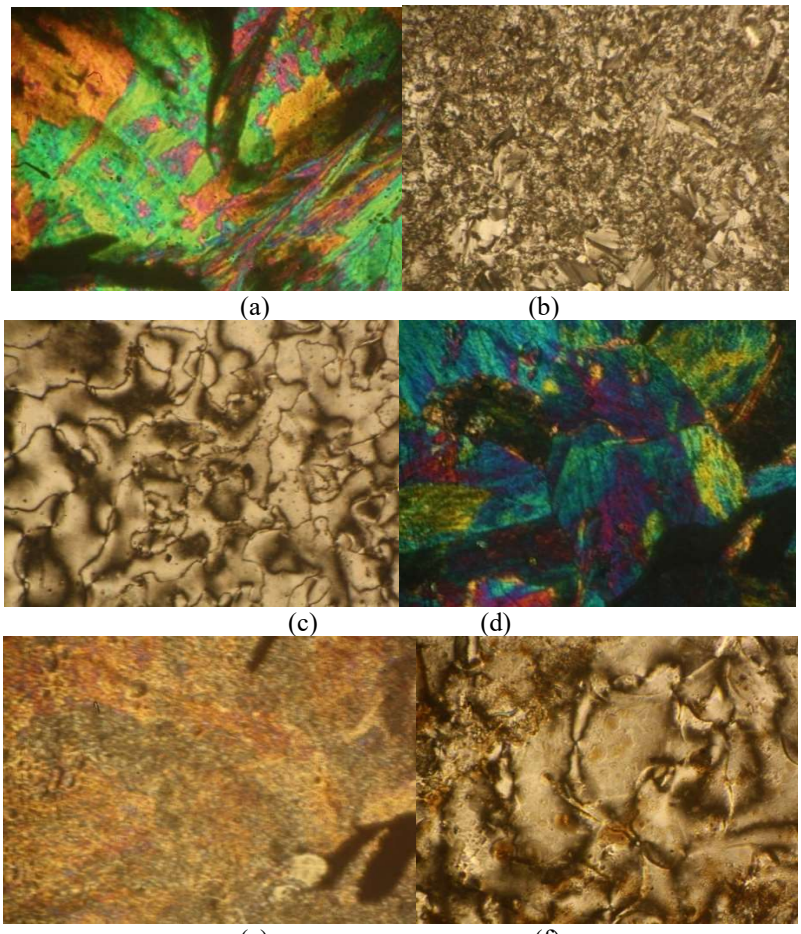

(a) (b)

(c) (d)

(e) (f)

Fig.-5: Optical Textures of Nano Doped (Fe_3O_4)4-*n*-Alkoxy benzoic acid (NnOBA, where n=7,8). (a) in Crystal Phase; (b) in Smectic A Phase; (c)in Nematic Phase of N7OBA, (d) in Crystal Phase; (e) in Cholesteric Phase; (f)in Nematic Phase of N8OBA

Colorimetry parameters: chromaticity coordinates and color purity of nOBA and NnOBA (where n = 7, 8) are measured from these optical textures using Eqs.6,7. The chromaticity coordinates and color purity of the pure and nano-doped liquid crystals in the crystal phase and in liquid crystalline phases such as the nematic, smectic A, and cholesteric phases are given in Table-3. The obtained chromaticity coordinates are compared with the standard chromaticity diagram shown in Fig.-6.[32,33]

Table-3: Chromacity Coordinates of nOBA and NnOBA in Different Phases

Compounds	Phase	Chromacity coordinates		Color purity (%)
		x	y	
nOBA	Cr	0.3172	0.378	….
	Sm /ch	0.442	0.475	85
	N	0.36	0.39	….
N7OBA	Cr	0.31	0.39	…
	Sm /ch	0.48	0.35	50
	N	0.47	0.35	50
N8OBA	Cr	0.39	0.4	…
	Sm/ch	0.44	0.35	72
	N	0.43	0.34	67

(Sm- Smectic A/C, ch-cholesteric, N-nematic, cr-crystal)

Table-3 demonstrates that color coordinates of nOBA and NnOBA (where n=7,8) in the crystalline phase and liquid crystalline phases are transparent for all wavelengths not contained in the narrow transmission peak for a single wavelength. The color coordinates of the crystalline phase are much closer to the white color coordinates (0.33,0.33), which means the textures of the sample in the crystalline phase appeared as different color composites. This was shown in the CIE 1931 chromaticity diagram in Fig.-6.

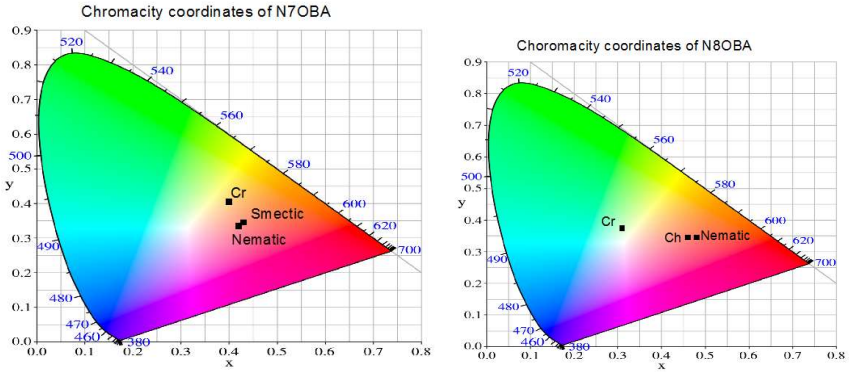

(a) (b)

Fig.-6: CIE 1931 Chromaticity Diagram of Nano Doped (Fe_3O_4) 4,n-alkoxy Benzoic Acid (NnOBA),(a) for N7OBA; (b)N80BA, (Cr – crystal; Ch: cholesteric)

The color purity of the samples is also presented in Table-3, where color purity is computed for the mesophase of the samples nOBA and NnOBA. The chromaticity coordinates of the mesophases of the samples (nOBA, NnOBA) are slightly nearer to the red color coordinates (0.529, 0.393).[33]Table-3 shows that the color purity of the N8OBA liquid crystal in mesophases is high compared to N7OBA. However, the color purity of nanocomposites is low compared to that of pure compounds. This is due to the fact that doping of the Fe_3O_4 nanoparticles in nOBA shields the dispersive forces and affects the orientation of the molecules at the surfaces. This reduces the birefringence (optical anisotropy) of the nanocomposites, which causes a reduction in color purity compared to pure nOBA. This kind of nanocomposites will be useful in other applications of liquid crystals, like healthcare and cosmetics, compared to display devices. The findings of the investigation reveal that analyzing the effects of nano dopants on liquid crystal properties requires a thorough examination of crystalline grain formation and grain boundaries. This can be achieved through techniques such as SEM imaging, X-ray diffraction measurements, and colorimetric parameters. The influence of Fe_3O_4 doping on structural, morphological, and colorimetric characteristics is more significant for 8OBA nanocomposites (N8OBA) compared to N7OBA.

CONCLUSION

Using X-ray diffraction and scanning electron microscopy techniques, the structural and morphological features of nano-doped liquid crystals, specifically 4, n-alkoxybenzoic acid (nOBA, where n = 7,8), doped with magnetic nanoparticles (Fe_3O_4), were effectively examined. Nonetheless, the structural parameters of X-ray diffraction patterns are very well acknowledged by the computed statistical parameters of SEM images. According to the investigation's findings, the doping of Fe_3O_4 nanoparticles has a significant impact on the structural and morphological characteristics of the 8OBA system.

ACKNOWLEDGEMENT

The authors are grateful to acknowledge M. R. College (A), Vizianagaram, A.P., The Gandhian Institute of Technology and Management (GITAM) deemed to be a University, Visakhapatnam, School of Sciences, Godavari Global University, Rajahmundry, A.P., for providing special assistance to do research work.

CONFLICT OF INTERESTS

The authors declare that there is no conflict of interest.

AUTHOR CONTRIBUTIONS

All the authors contributed significantly to this manuscript, participated in reviewing/editing and approved the final draft for publication. The research profile of the authors can be verified from their ORCID ids, given below:

Sowmya Mudunuru https://orcid.org/0009-0005-5022-4306
Ganapavarapu Veera Raghava Sharma https://orcid.org/0000-0002-4550-0979
Chandra Sekhara Rao Gurubilli https://orcid.org/0009-0004-8955-8672
Srinivas Rao G. https://orcid.org/0000-0001-9647-7206
Gowri Sankara Rao B. http://orcid.org/0000-0002-7856-5816

REFERENCES

1. C. N. R. Rao, A. Muller, A. K. Cheetham, The Chemistry of Nanomaterials: Synthesis, Properties and Applications; Wiley-VCH: Weinheim, Germany, 2006.
2. M. S. Chavali, M. P. Nikolova, *SN Applied Sciences*, **1(607)**, 1(2019), https://doi.org/10.1007/s42452-019-0592-3
3. B. D. Mattos, B. L. Tardy, W. L. E. Magalhães, O. J. Rojas, *Journal of Controlled Release*, **262**, 139(2017), https://doi.org/10.1016/j.jconrel.2017.07.025
4. S. Kumar, H. K. Bisoyi, *Angewandte Chemie International Edition,* **46(9)**, 1501(2007), https://doi.org/10.1002/anie.200603967.
5. A. Gowda, S. Kumar, *Materials*, **11(3)**, 382, 1(2018), https://doi.org/10.3390/ma11030382
6. A. B. Shivanandareddy, V. Krishnamurthy, V. Lakshminarayanan, S. Kumar, *Chemical Communications*, **50**, 710(2014), http://dx.doi.org/10.1039/c3cc47685e
7. C. Burda, X. Chen, R. Narayanan, M. A. El-Sayed, *Chemical Reviews*, **105(4)**, 1025(2005), http://dx.doi.org/10.1021/cr030063a
8. Daniel, M.-C.; Astruc, D. *Chemical Reviews*, **104(1)**, 293(2004), http://dx.doi.org/10.1021/cr030698+
9. H. Nguyen, T.D. T. Ung, T. H. Vu, T. K. C. Tran, V. Q. Dong, D. K. Dinh, Q. L. Nguyen, *Advances in Natural Sciences Nanoscience and Nanotechnology*, **3(3)**, 035014(2012), http://dx.doi.org/10.1088/2043-6262/3/3/035014
10. L. Scolari, G. Sebastian, X. Haiqing, Lei Zhai, E. Lars, T. A. Thomas, T. W. Shin, B. Anders, *AIP Conference Proceedings*, **1055**, 29(2008), http://dx.doi.org/10.1364/WSOF.2008.OSD29
11. M. Kumar, S. Kumar, *RSC Advances*, **5(2)**, 1262(2015), http://dx.doi.org/10.1039/C4RA12211A

12. L. Bing, Y. Tao, M. Xin, M. Zhijian, L. Hao, W. Yao, Z. Guofu, *Nanomaterials*, **11(2)**, 448(2021), https://doi.org/10.3390/nano11020448
13. J. P. F. Lagerwall, G. Scalia, *Current Applied Physics*, **12(6)**, 1387(2012), http://dx.doi.org/10.1016/j.cap.2012.03.019
14. P. Yaduvanshi, S. Kumar, R. Dhar, *Phase Transitions*, **88(5)**, 88, 489(2014), http://dx.doi.org/10.1080/01411594.2014.984710
15. A. G. Maria, L. Nefeli, V. A. Ioanna, G. Maria, P. A. Evangelia, *Nanomaterials*, **13**, 122(2022), https://doi.org/10.3390/nano13010122
16. Y. Shen, I. Dierking, *Applied Sciences*. **9(12)**, 2512(2019), http://dx.doi.org/10.3390/app9122512
17. N. Manjula, M. Pugalenthi, V. S. Nagarethinam, K. Usharani, A. R. Balu, *Material Science – Poland,* **33(4)**,774(2015), http://dx.doi.org/10.1515/msp-2015-0115
18. S. M. John, D. Dietrich, G. John, G. W. George, H. W. Spiess, V. Volkmar, *Handbook of Liquid Crystals: Fundamentals*, **1**, 635(2008), http://dx.doi.org/10.1002/9783527620760.ch8c
19. L. M. Blinov, Liquid Crystals: X-ray Liquid Crystal Structure Analysis
20. M. Tuceryan, A.K. Jain, Texture analysis-*The Handbook of Pattern and Computer Vision,***2**, 207(1998).
21. R. C. Gonzalez, R. E. Woods; S. L. Eddins, *Digital Image Processing Using MATLAB,* Dorling Kindersley (India) Pvt. Ltd., Delhi, 2004.
22. J. Liang, S.Liang ling, G. Annadurai, D. Balaji, W. Shaoying, Qi Sun, Q. Jialei, G. Heng, B. Li, H. Xiaoyong, *RSC Advances*, **8**, 32111(2018),https://doi.org/10.1039/C8RA06129G
23. Janos Schanda, CIE Chromaticity Diagrams, CIE Purity, CIE Dominant Wavelength, University of Pannonia, Veszprém, Hungary
24. H. Araki, J. Kim, S. Zhang, A. Banks, K. Crawford, X. Sheng, P. Gutruf, Y. Shi, R. M. Pielak, J. A. Rogers, *Advanced Functional Materials*, **27(2)**, 1(2017), https://doi.org/10.1002/adfm.201604465
25. Y. A. Elif, P. Yasemin, E. Digdem, K. Ahmet, B. Bahadir, U. Huseyin, y. Gonul, D. Neslihan, Y. Mustafa, E. Ayhan, *Physica Scripta*, **98(8)**, 085409(2023), https://doi.org/10.1088/1402-4896/ace806
26. S. Singh, M. Singh, Proceedings of the 2004 IEEE International Conference on Computational Intelligence for Homeland Security and Personal Safety, 2004. CIHSPS 2004. https://doi.org/10.1109/CIHSPS.2004.1360196
27. Ingo Dierking, Textures of Liquid Crystals, Wiley-Vch, 2003.
28. Fritz Albregtsen, *Ph.D.Thesis: Statistical Texture Measures computed from Gray Level CooccurrenceMatrices,* Image Processing Laboratory, Department of Informatics, University of Oslo, 2008.
29. https://stackoverflow.com/questions/15566063/what-exactly-is-edge-density
30. H. E. Swanson, H. F. McMurdie, M. C. Morris, and E. H. Evans, Standard X-ray Diffraction Powder Patterns, https://nvlpubs.nist.gov/nistpubs/Legacy/MONO/nbsmonograph25-5.pdf
31. A. A. A. Ramiz, *IOSR Journal of Applied Physics,* **8**, 6(2016).
32. https://www.rp-photonics.com/chromaticity.html
33. C. A. Bouman, Digital Image Processing, 2024, https://engineering.purdue.edu/~bouman/ece637/notes/pdf/ColorSpaces.pdf
34. M. Sowmya, G. C. S. Rao, G. V. R. Sharma, G. S. Rao, B. G. S. Rao, *Rasayan Journal of Chemistry*, **17(1)**, 1(2024), http://doi.org/10.31788/RJC.2024.1718680
35. J. Sivasri, M. C. Rao, G. Giridhar, B. T. P. Madhav, T. E. Divakar, R. K. N. R. Manepalli, *Rasayan Journal of Chemistry*, **9(4)**, 556(2016).

[RJC- 8868/2024]